

Brownian yet non-Gaussian diffusion in heterogeneous systems

E. B. Postnikov

Department of Theoretical Physics, Kursk State University, Radishcheva st., 33, 305000 Kursk, Russia

A. Chechkin

*Institute of Physics and Astronomy, Potsdam University,
Karl-Liebknecht-Strasse 24/25, 14476 Potsdam-Golm, Germany and
Akhiezer Institute for Theoretical Physics, Akademicheskaya Str. 1, 61108 Kharkov, Ukraine*

I.M. Sokolov*

Institut für Physik and IRIS Adlershof, Humboldt Universität zu Berlin, Newtonstraße 15, 12489 Berlin, Germany

We discuss the situations under which Brownian yet non-Gaussian (BnG) diffusion can be observed in the model of a particle's motion in a random landscape of diffusion coefficients slowly varying in space. Our conclusion is that such behavior is extremely unlikely in the situations when the particles, introduced into the system at random at $t = 0$, are observed from the preparation of the system on. However, it indeed may arise in the case when the diffusion (as described in Ito interpretation) is observed under equilibrated conditions. This paradigmatic situation can be translated into the model of the diffusion coefficient fluctuating in time along a trajectory, i.e. into a kind of the “diffusing diffusivity” model.

Many experiments in different complex systems point onto a wide-spread (if not universal) behavior of displacements of tracers termed Brownian yet non-Gaussian (BnG) diffusion [1]: The mean squared displacement (MSD) of the tracers grows linearly in time, $\langle \mathbf{x}^2 \rangle = 2dD_0t$, (with D_0 being the diffusion coefficient and d being the dimension of space) like in the normal, Fickian diffusion; the probability density function (PDF) of the displacements is, however, strongly non-Gaussian. At short times the PDF often approximately follows the two-sided exponential (Laplace) pattern.

This type of behavior may stem from the heterogeneity of tracers [2–4], each of them having its own diffusion coefficient in a homogeneous environment. In the majority of cases the form of the PDF changes at larger times for the normal, Gaussian one, see [5–8]. Such change cannot be described within the tracers' heterogeneity model unless the properties of tracers change in time. The exponential-to-Gaussian transition in the PDF may stem from temporal fluctuations of the diffusion coefficient of tracers or of the medium (a “diffusing diffusivity” model [9–13]), or from the spacial inhomogeneity of the medium, as mentioned in [11]. In this case at short times different tracers see different diffusion coefficients (“superstatistics”, [14]), while at long times (and correspondingly large scales) the homogenization sets in, and the motion of each tracer can be described as taking place in a homogeneous medium characterized by some effective diffusion coefficient D^* .

The BnG diffusion implies that the diffusion coefficient sampled at short times is equal to the effective one in the homogenized regime. The topic of the present discussion is to find out when this is likely to be the case.

In order to observe heterogeneity at short times the local diffusion coefficient $D(\mathbf{x})$ has to vary only slowly

in space. The correlation length λ of $D(\mathbf{x})$ is therefore mesoscopic, and the characteristic time of the transition from the short time inhomogeneous (superstatistical) to the homogenized behavior is $t_H \sim \lambda^2/D_0$. In dimensions higher than $d = 1$ our system will be assumed to be isotropic on the average. This is the case not in all, but in the most of the situations observed experimentally. The assumption of isotropy simplifies the further discussion considerably.

In heterogeneous media, the situations under equilibrium, and the non-equilibrium ones may show very different properties due to (weak) ergodicity breaking [15, 16]. The first, equilibrium, situation corresponds to the case when the system (medium, already containing tracers) was prepared long before starting the observation. The position of the tracer is monitored from the beginning of observation ($t = 0$) on. If there are several tracers in the system, the ones to observe are chosen at random. In this case the probability density to find a tracer at position \mathbf{x} at $t = 0$ is proportional to the equilibrium density $n(\mathbf{x})$ of tracers at the corresponding position. If $n(\mathbf{x})$ is not constant, the space is not sampled homogeneously. The second, opposite, situation corresponds to the case when the tracers were introduced at random exactly at the beginning of the observation, and the diffusivity landscape is sampled homogeneously. We will call the first and the second situations the *equilibrium sampling*, and the *homogeneous sampling*, respectively. In most of the experiments and simulations on BnG diffusion a moving time averaging over the long data acquisition time is used to get both the displacement's PDFs and the MSDs, so that the system has enough time to equilibrate. In [5] the ensemble average was used, but time between preparation and the beginning of the observation was not specified. The situation will be equilibrated if this time is larger

than t_H .

The knowledge of the diffusion coefficient $D(\mathbf{x})$ as a function of the coordinates is not enough to uniquely define the properties of this diffusion. Systems with exactly the same $D(\mathbf{x})$, the ones described by the Langevin equation $\dot{\mathbf{x}} = \mu(\mathbf{x})\mathbf{f}(\mathbf{x}) + \sqrt{2D(\mathbf{x})}\boldsymbol{\xi}(t)$ with $\mathbf{f}(\mathbf{x})$ being the deterministic force, and with the noise $\boldsymbol{\xi}(t)$ fulfilling $\langle \boldsymbol{\xi} \rangle = 0$ and $\langle \xi_\beta(t)\xi_\gamma(t') \rangle = \delta_{\beta\gamma}\delta(t-t')$ with β, γ denoting Cartesian components, are described by different Fokker-Planck equations (FPEs), depending on what interpretation of the stochastic integral is assumed. In what follows we concentrate on the case $\mathbf{f} = 0$. The corresponding FPEs for a given realization of $D(\mathbf{x})$ read $\frac{\partial P(\mathbf{x}, t)}{\partial t} = \nabla[(1-\alpha)\nabla D(\mathbf{x}) + D(\mathbf{x})\nabla]P(\mathbf{x}, t)$, with the interpretation parameter α taking the values on the interval $0 \leq \alpha \leq 1$. The typical interpretations, the Ito, Stratonovich and the Hänggi-Klimontovich (HK) ones, correspond to $\alpha = 0, 1/2$ and 1 , respectively. The equilibrium concentration profile $n(\mathbf{x}) \propto P(\mathbf{x}, t \rightarrow \infty)$ corresponding to the vanishing flux in a closed system is given by the solution of the equation $(1-\alpha)n(\mathbf{x})\nabla D(\mathbf{x}) + D(\mathbf{x})\nabla n(\mathbf{x}) = 0$ and reads

$$n(\mathbf{x}) = CD^{\alpha-1}(\mathbf{x}) \quad (1)$$

with C being the integration constant. The HK case is the only one when this profile is flat. The Fokker-Planck equation for HK case corresponds to the phenomenological second Fick's law $\frac{\partial n(\mathbf{x}, t)}{\partial t} = \nabla[D(\mathbf{x})\nabla n(\mathbf{x}, t)]$. The Ito interpretation leads to the Fokker-Planck equation $\frac{\partial n(\mathbf{x}, t)}{\partial t} = \Delta[D(\mathbf{x})n(\mathbf{x}, t)]$, which, in some cases, better reproduces the experimental results for heterogeneous diffusion and is connected with the continuous time random walk (CTRW) scheme [17].

Sampled diffusion coefficient distributions. The PDF of particles' displacements $p(\mathbf{x}, t)$ follow from $P(\mathbf{x}, t)$ for given $D(\mathbf{x})$ via averaging over the realizations of the diffusivity landscapes. Let us take as a "stylized fact" that the PDF of displacements at short times has the exponential form

$$p(\mathbf{x}, t) = C(t) \exp(-a(t)|\mathbf{x}|), \quad (2)$$

with time dependent parameters $a(t)$ and $C(t)$ which follow from the requirements that $\int p(\mathbf{x}, t)d\mathbf{x} = 1$ and that $\int p(\mathbf{x}, t)|\mathbf{x}|^2 d\mathbf{x} = 2dD_0t$ (see [18] for the explicit expressions in $d = 1, 2$ and 3). The PDF of the particles' displacements in the superstatistical regime (when each particle can be considered as moving with its own diffusion coefficient K) is given by

$$p(\mathbf{x}, t) = \int_0^\infty \frac{1}{(4\pi dKt)^{d/2}} \exp\left(-\frac{x^2}{2dKt}\right) p_K(K) dK \quad (3)$$

where $p_K(K)$ is the PDF of sampled diffusion coefficients. This is defined by Eq.(12) and may or may not be equal to the one-point PDF $p_D(D)$ of the random field $D(\mathbf{x})$.

Passing to the Fourier transform in \mathbf{x} and taking into account the isotropy of $p(\mathbf{x}, t)$ we get $\tilde{p}(\mathbf{k}, t) = \int_0^\infty \exp(-Ktk^2) p_K(K) dK$, and see that $\tilde{p}(k, t)$ is the Laplace transform of $p_K(K)$ taken at the value of the Laplace variable $s = tk^2$. Thus, $p_K(K)$ follows by the inverse Laplace transform [18] and is a Γ -distribution.

In situations corresponding to homogeneous sampling, the two PDFs, $p_D(D)$ and $p_K(K)$ coincide, so that $p_D(D)$ is given by

$$p_D(D) = \frac{\beta^\beta}{\Gamma(\beta)} \frac{1}{\bar{D}} \left(\frac{D}{\bar{D}}\right)^{\beta-1} \exp\left(-\beta \frac{D}{\bar{D}}\right) \quad (4)$$

with

$$\beta = \frac{d+1}{2}, \quad \bar{D} = D_0. \quad (5)$$

The same is true also for equilibrated HK case, when the concentration profile given by Eq.(1) is flat.

The situation in other equilibrated cases is different. In these cases the probability density to find a domain with diffusivity D by picking up a particle at random (i.e. to have $K = D$ for the particle's diffusion coefficient) is proportional to $np(n, D)$ where $p(n, D)$ is the joint probability density of $n(\mathbf{x})$ and $D(\mathbf{x})$. Thus $p_K(D) = N \int_0^\infty np(n, D) dn$, where the normalization constant is given by $N = [\int_0^\infty \int_0^\infty np(n, D) dn dD]^{-1} = [\int_0^\infty \langle n|D \rangle p_D(D) dD]^{-1}$, with $\langle n|D \rangle$ being the first conditional moment of the concentration. The PDF $p_D(D)$ appears now as a marginal PDF of local diffusivities, $p_D(D) = \int_0^\infty p(n, D) dn$. Thus N is the inverse of the ensemble mean concentration, which coincides with a volume mean in the thermodynamical limit: $N = \langle n(\mathbf{x}) \rangle^{-1}$. Introducing the dimensionless concentration $\nu(\mathbf{x}) = Nn(\mathbf{x}) = n(\mathbf{x})/\langle n(\mathbf{x}) \rangle$ we may write

$$p_K(D) = \int_0^\infty \nu p(\nu, D) d\nu = \langle \nu|D \rangle p_D(D). \quad (6)$$

According to our definition $\langle \nu(\mathbf{x}) \rangle = 1$ provided the corresponding mean exists. Therefore if $p_D(D)$ is normalized, so is also $p_K(K)$ since $\int_0^\infty \langle \nu|D \rangle p_D(D) dD = \langle \nu \rangle = 1$. According to Eq.(1) the connection between $n(\mathbf{x})$ and $D(\mathbf{x})$ is deterministic, so that $N = \langle D^{\alpha-1}(\mathbf{x}) \rangle^{-1}$. Now we can write $\langle \nu|D \rangle = \nu(D) = ND^{\alpha-1}(\mathbf{x})$, substitute this in Eq.(6) and require the normalization. Then the PDF $p_D(D)$ follows in form of the Γ -distribution Eq.(14), see [18] for details, with parameters

$$\beta = \frac{d+3}{2} - \alpha, \quad \bar{D} = \frac{d+3-2\alpha}{d+1} D_0. \quad (7)$$

Homogenized behavior. Now let us consider the long-time behavior of the diffusion coefficient corresponding to its homogenization. At long times particles sample large domains of the system and feel some effective diffusion coefficient D^* . The value of D^* can be obtained considering

a stationary situation, e.g. measuring the stationary flow through a large piece of the medium with concentrations kept constant at its boundaries [19]. The homogenization of the diffusion coefficient in a heterogeneous medium is similar to the one for the electric conductivity, with one important difference discussed below. For the case of the conductivity we have $\mathbf{E}(\mathbf{x}) = -\text{grad } \phi$ (with $\text{rot } \mathbf{E} = 0$) and $\mathbf{j}(\mathbf{x}) = \sigma(\mathbf{x})\mathbf{E}(\mathbf{x})$ (with $\text{div } \mathbf{j} = 0$), i.e. homogenize the equation $\nabla[\sigma(\mathbf{x})\nabla\phi] = 0$ with the given potential on the boundaries. The effective value σ^* follows from the condition that the heat production in the homogeneous system described by $\nabla[\sigma^*\nabla\phi] = 0$ is the same as in the heterogeneous one, or that the mean values of the electric fields in both systems coincide [20, 21]. This scheme corresponds to homogenization of the phenomenological Fick's law, but not to the general FPE.

Let us assume, we are able to calculate the effective conductance σ^* of an inhomogeneous system with the local conductances $\sigma(\mathbf{x})$ and denote this as a special type of an average, the homogenization mean, by $\sigma^* = \langle\sigma(\mathbf{x})\rangle_H$. Then the effective diffusion coefficient in the homogenized regime for the general diffusive case is given by the same type of the average:

$$D^* = \frac{\langle D(\mathbf{x})n(\mathbf{x}) \rangle_H}{\langle n(\mathbf{x}) \rangle} = \langle D(\mathbf{x})\nu(\mathbf{x}) \rangle_H = \langle \kappa \rangle_H, \quad (8)$$

where $\kappa(\mathbf{x}) = D(\mathbf{x})\nu(\mathbf{x})$, as shown in [19]. An alternative proof can follow the lines of [22]. A simple physical explanation (not following the lines of the proofs) is as follows.

Let the tracers carry a charge q , and move in electric field \mathbf{E} under the force $\mathbf{f} = q\mathbf{E}$. Then the local current density is $\mathbf{j}(\mathbf{x}) = q^2 n(\mathbf{x})\mu(\mathbf{x})\mathbf{E}(\mathbf{x})$, with $\mu(\mathbf{x}) = D(\mathbf{x})/k_B T$ being the local mobility, giving $\sigma(\mathbf{x}) = q^2 D(\mathbf{x})n(\mathbf{x})/k_B T$. Now we calculate the large scale conductance σ^* and assume that it is connected with the homogenized diffusion coefficient and the mean density by the same Nernst-Einstein relation $\sigma^* = q^2 D^* \langle n(\mathbf{x}) \rangle / k_B T$. From this we get Eq.(8).

The homogenized conductance possesses the upper and the lower bound, from which the Wiener bounds, see e.g. [20], are the most general (and loose) ones:

$$\langle \sigma^{-1}(\mathbf{x}) \rangle^{-1} \leq \langle \sigma(\mathbf{x}) \rangle_H \leq \langle \sigma(\mathbf{x}) \rangle. \quad (9)$$

The averages in the bounds in Eq.(9) can be considered either as volume or as ensemble means.

In $d = 1$ the homogenization mean corresponds *exactly* to the lower bound

$$\langle \sigma(x) \rangle_H = \langle \sigma^{-1}(x) \rangle^{-1}, \quad (10)$$

which follows immediately from the Ohm's law. In dimensions $d > 1$ the optimal bounds (i.e. the equalities) in Eq.(9) are realized in layered systems, which are ruled out by the isotropy. However the inequalities of

the Hashin-Shtrikman type (assuming isotropy), see e.g. [23], do not lead to tighter bounds as long as the local values of D are not bounded away from zero and infinity.

Far from percolation transition σ^* is typically well reproduced by the effective medium approximation (EMA), see [21] for the discussion. Within this approximation $D^* = \langle \kappa \rangle_H$ is given by the solution of the equation

$$\left\langle \frac{D^* - \kappa}{(d-1)D^* + \kappa} \right\rangle = 0, \quad (11)$$

where the average again can be considered either as a volume average or as an average over the distribution of κ . We note that for $d = 1$ EMA reproduces the exact result, Eq.(10). Eq.(11) is pertinent to quadratic and cubic lattices in $d = 2$ and 3 [24], and to continuous d -dimensional systems [21]. When the PDF $p(\kappa)$ is known, Eq.(11) can be solved numerically for D^* .

Systems with homogeneous equilibrium. In the HK case (the random diffusivity model of Ref.[22]) $\nu(\mathbf{x}) = 1$, and the distributions of κ and of K coincide. The upper Wiener bound corresponds to $D^* = D_0$. The result of EMA from Eq.(11) is $D^* = 0.719D_0$ in $d = 2$ and $D^* = 0.852D_0$ in $d = 3$, both smaller than D_0 . In $d = 1$ the first inverse moment $\int_0^\infty K^{-1}p(K)dK$ of the PDF Eq.(14) diverges, and the effective diffusion coefficient D^* vanishes, giving rise to anomalous diffusion [19].

Independently on the quality of approximation given by EMA we note that the EMA result is realizable in the continuum case [25]: the ensemble of all “disordered” configurations contains realizations with the effective conductance equal to the one predicted by EMA. The lower Wiener bounds, corresponding to $\frac{1}{3}D_0$ and $\frac{1}{2}D_0$ in $d = 2$ and 3 , are also realizable. Therefore situations leading to the BnG diffusion are highly unlikely because the ensemble of disordered systems should contain the realizations with diffusivities close to the upper *and* to the lower bound, as well as the ones given by EMA, and the fact that the last two are underrepresented should have some generic grounds, which are hard to find.

As an example of the time dependence of the diffusion coefficient in the HK case we present in Fig. 1 the results of simulations in $d = 2$. The figure shows $D(t) = \frac{d}{dt} \langle x^2(t) \rangle$ normalized on D_0 . The details of our simulation approach are given in [18]. One readily infers that the diffusion coefficient decays with time, so that no BnG diffusion is observed. The value of the terminal diffusion coefficient D^* as obtained in simulations agrees well with the EMA prediction. For systems with homogeneous equilibrium there is no difference between equilibrium and homogeneous sampling situations.

Systems with inhomogeneous equilibrium. For systems with inhomogeneous equilibrium the two situations are different. We start our discussion using the hints given by the EMA.

Let us start from the case of homogeneous sampling. In this case the equilibrium reduced density $\nu(\mathbf{x}) =$

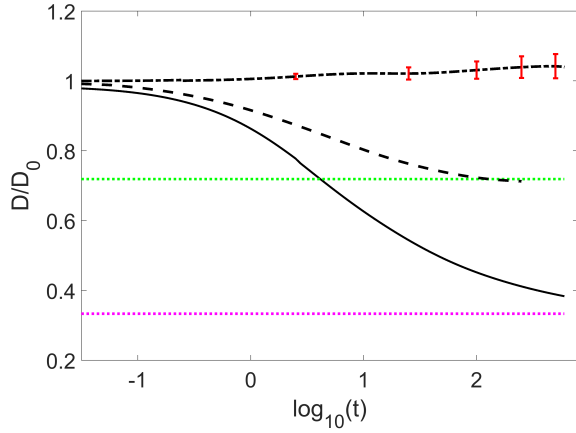


FIG. 1. The behavior of $D(t)/D_0$ for the HK case and the two Ito cases for the same value of $\lambda = 10$ in $d = 2$. The upper dashed-dotted line corresponds to the equilibrated Ito case and stays horizontal within the statistical error. The error bars show standard deviations of the mean in 1500 realizations. The lower dashed line gives the time-dependent diffusion coefficient in the HK case. The lowest full line corresponds to the Ito situation under homogeneous sampling. For these lines the statistical errors are of the order of the lines' thickness. The dotted thin lines correspond to asymptotic predictions of Fig. 2.

$D^{\alpha-1}(\mathbf{x})\langle D^{\alpha-1}(\mathbf{x}) \rangle^{-1} = \frac{\beta^{\alpha-1}\Gamma(\beta)}{\Gamma(\beta+\alpha-1)} D^{\alpha-1} D_0^{1-\alpha}$ [18]. The distribution of $\kappa = D^\alpha / \langle D^{\alpha-1} \rangle$ follows from $p_D(D)$ by the variable transformation. Applying it in Eq.(11) we get D^* as a function of α . The quotient D/D_0 as a function of α is shown in Fig. 2 for $d = 2$ as the lower curve. We see that the difference between the short time diffusion coefficient D_0 and the long-time one D^* increases when α decreases from 1. Parallel to the discussion above, there is no reason to await for BnG behavior.

In the equilibrated case the parameters of the distribution $P_D(D)$ are given by Eq.(7), and the normalization constant reads $N = \frac{[(d+1)/2]^{\alpha-1}\Gamma[(d+1)/2-\alpha]}{\Gamma[(d+1)/2]} D_0^{1-\alpha}$, see [18]. The PDF of κ again follows by the variable transformation. The result of EMA for this, equilibrated, case is shown in Fig. 2 as the upper curve. We see that the behavior of the equilibrated system is opposite to the one for homogeneous sampling, and that for $\alpha \rightarrow 0$ the difference between D^* and D_0 vanishes. This is not an artifact of the approximation, but a true physical effect.

For $\alpha = 0$ the normalization constant is $N = D_0$ in all dimensions, and $\nu = D_0/D$. Therefore $\kappa = D_0$ does not fluctuate, and $\langle \kappa \rangle_H = D_0$ coincides with the short-time sampled diffusion coefficient. Contrary to the previous case, this behavior persists even in $d = 1$, see [18]. The simulation results for the Ito cases are shown in Fig. 1 along with the one for the HK case.

Fig. 3 displays the PDFs for equilibrated Ito case at different times. These exhibit the transition from expo-

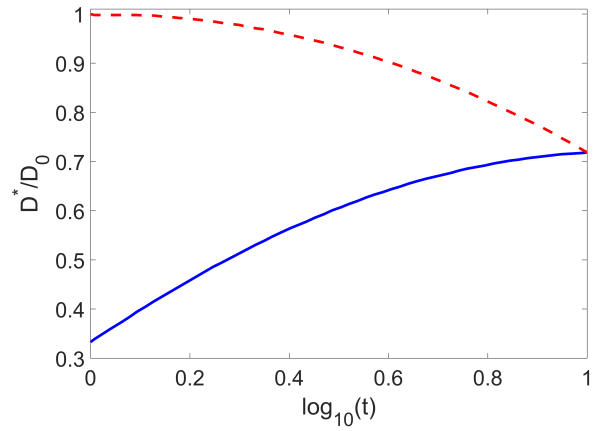


FIG. 2. The EMA predictions for the values of D^*/D_0 in $d = 2$ as a function of the parameter α defining the interpretation. The upper (dashed) curve represents the results for the equilibrated case, the lower (full) one for the case of homogeneous sampling.

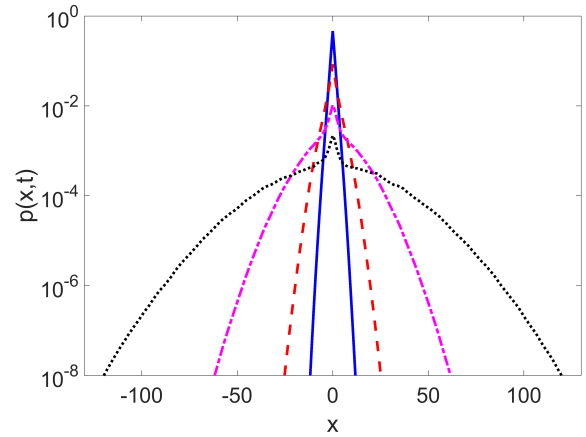


FIG. 3. The PDFs in the equilibrated Ito case for $t = 1, 10, 100$ and 500 . The figure demonstrates the transition between the double-sided exponential and the Gaussian form in a BnG situation.

nential to a Gaussian distribution, showing a pronounced central peak at intermediate times, which is well known from the experimental realizations [5, 6, 26], as well as from other models [27, 28].

The Ito interpretation relies on the martingale property, which, in the Gaussian case, means that the increments of the process for small times are symmetric. Taking time increments fixed leads to a random walk with locally symmetric steps, in which the spatial change of the diffusivity has to be attributed to waiting times changing in space. Such a random walk scheme corresponds to a trap model [29] which is thus the most prominent candidate for modeling BnG diffusion. In higher dimensions (in $d = 3$ and in $d = 2$ up to logarithmic corrections which are hard to detect) trap models may be mapped to

CTRW as their continuous (homogenized) limit [30], i.e. to the models subordinated to simple random walk, see e.g. [31], with the diffusing diffusivity model [11] being a representative of the class.

Conclusions. Taking into account all said above we conclude that the only promising candidate for explanation of the BnG diffusion in random diffusivity landscapes is the equilibrated trap (Ito) model, which in higher dimensions can be translated into the diffusive diffusivity model. For all other cases observing the effect is extremely unlikely.

Acknowledgement. EBP is supported by the Russian Science Foundation, project 16-15-10252. AC acknowledges the support by the Deutsche Forschungsgemeinschaft within the project ME1535/6-1.

* igor.sokolov@physik.hu-berlin.de

- [1] R. Metzler, Gaussianity Fair: The Riddle of Anomalous yet Non-Gaussian Diffusion, *Biophysical Journal* **112** 1 (2017)
- [2] S.J. Park, S. Song, I.-C. Jeong, H.R. Koh, J.-Hy. Kim, and J. Sung, Nonclassical Kinetics of Clonal yet Heterogeneous Enzymes, *J. Phys. Chem. Lett.* **8** 3152 (2017)
- [3] S. Petrovsky, A. Morozov, Dispersal in a Statistically Structured Population: Fat Tails Revisited, *The American Naturalist* **173** 279 (2009)
- [4] O. Sliusarenko, S. Vitali, V. Sposini, A. Chechkin, G. Castellani, and G. Pagnini, Finite-energy Levy-type motion through heterogeneous ensemble of Brownian particles, arXiv:1807.07883
- [5] B. Wang, S.M. Antony, S.C. Bae and S. Granick, Anomalous yet Brownian, *PNAS* **106** 15160 (2009)
- [6] B. Wang, J. Kuo, S.C. Bae and S. Granick, When Brownian diffusion is not Gaussian, *Nature Materials* **11** 481 (2012)
- [7] S. Hapca, J.W. Crawford, and I.M. Young, Anomalous diffusion of heterogeneous populations characterized by normal diffusion at the individual level, *J. R. Soc. Interface* **6**, 111122 (2009)
- [8] S. Bhattacharya, D.K. Sharma, S. Saurabh, S. De, A. Sain, A. Nandi, and Arindam Chowdhury, Plasticization of Poly(vinylpyrrolidone) Thin Films under Ambient Humidity: Insight from Single-Molecule Tracer Diffusion Dynamics, *J. Phys. Chem. B* **117** 7771 (2013)
- [9] M.V. Chubynsky and G.W. Slater, Diffusing Diffusivity: A Model for Anomalous, yet Brownian, Diffusion, *Phys. Rev. Lett.* **113**, 098302 (2014)
- [10] R. Jain and K.L. Sebastian, Diffusion in a Crowded, Rearranging Environment, *J. Phys. Chem. B* **120**, 3988 (2016)
- [11] A.V. Chechkin, F. Seno, R. Metzler, I.M. Sokolov, Brownian yet non-Gaussian diffusion: from superstatistics to subordination of diffusing diffusivities, *Phys. Rev. X* **7** (2) 021002 (2017)
- [12] N. Tyagi and B.J. Cherayil, Non-Gaussian Brownian Diffusion in Dynamically Disordered Thermal Environments, *J. Phys. Chem. B* **121**, 7204 (2017)
- [13] Y. Lanoiselée and D.S. Grebenkov, A model of non-Gaussian diffusion in heterogeneous media, *J. Phys. A: Math. Theor.* **51** 145602 (2018)
- [14] C. Beck, Superstatistical Brownian Motion, *Prog. Theor. Phys. Suppl.* **162**, 29 (2006)
- [15] R. Metzler, J.-H. Jeon, A. G. Cherstvy, and E. Barkai, Anomalous diffusion models and their properties: non-stationarity, non-ergodicity, and ageing at the centenary of single particle tracking, *Phys. Chem. Chem. Phys.* **16** 24128 (2014)
- [16] Y. Meroz, I.M. Sokolov, A toolbox for determining subdiffusive mechanisms, *Physics Reports* **573** 1-29 (2015)
- [17] B.Ph. van Milligan, P.D. Bons, B.A. Carreras, and R. Sánchez, On the applicability of Fick's law to diffusion in inhomogeneous systems, *Eur. J. Phys. B* **26** 913 (2005)
- [18] See supplemental material available online. It contains the explicit calculations for the distributions of local diffusivities and the corresponding normalization constants, details and results of numerical simulations of MSD and PDF for different cases discussed in the main text.
- [19] F. Camboni and I.M. Sokolov, Normal and anomalous diffusion in random potential landscapes, *Phys. Rev. E* **85**, 050104 (2012)
- [20] M.J. Beran, *Statistical Continuum Theories*, Wiley, N.Y. 1968
- [21] M. Sahimi, *Heterogeneous Materials*, Vol.1 Linear transport and Optical Properties, Springer, N.Y., 2003
- [22] D.S. Dean, I.T. Drummond and R.R. Horgan, Effective transport properties for diffusion in random media, *J. Stat. Mech.: Theor. and Exp.*, P07013 (2007).
- [23] D.C. Pham and S. Torquato, *J. Appl. Phys.* **94**, 6591-6602 (2003)
- [24] S. Kirkpatrick, Percolation and conductivity, *Rev. Mod. Phys.* **45**, 574 (1973)
- [25] G.W. Milton, The coherent potential approximation is a realizable effective medium scheme, *Comm. Math. Phys.* **99**, 463-500 (1985)
- [26] C.E. Wagner, B.S. Turner, M. Rubinstein, G.H. McKinley, and K. Ribbeck, A Rheological Study of the Association and Dynamics of MUC5AC Gels, *Biomacromolecules* **18**, 3654-3664 (2017)
- [27] L. Luo and M. Yi, Non-Gaussian diffusion in static disordered media, *Phys. Rev. E* **97**, 042122 (2018)
- [28] S. Stylianidou, T.J. Lampo, A.J. Spakowitz, and P.A. Wiggins, Strong disorder leads to scale invariance in complex biological systems, *Phys. Rev. E* **97**, 062410 (2018)
- [29] I.M. Sokolov, Ito, Stratonovich, Hänggi and all the rest: The thermodynamics of interpretation, *Chemical Physics* **375**, 359-363 (2010)
- [30] J. Klafter and R. Silbey, Derivation of the Continuous-Time Random-Walk Equation, *Phys. Rev. Lett.* **44** 55 (1980)
- [31] J. Klafter and I.M. Sokolov, *First Steps in Random Walks: From tools to Applications*, Oxford Univ. Press, Oxford, 2011.

Brownian yet non-Gaussian diffusion in heterogeneous systems

Supplemental material

E. B. Postnikov

Department of Theoretical Physics, Kursk State University, Radishcheva st., 33, 305000 Kursk, Russia

A. Chechkin

Institute of Physics and Astronomy, Potsdam University, Karl-Liebknecht-Strasse 24/25, 14476 Potsdam-Golm, Germany

Akhiezer Institute for Theoretical Physics, Akademicheskaya Str. 1, 61108 Kharkov, Ukraine

I.M. Sokolov

Institut für Physik and IRIS Adlershof, Humboldt Universität zu Berlin, Newtonstraße 15, 12489 Berlin, Germany

DISTRIBUTIONS OF SAMPLED DIFFUSION COEFFICIENTS AND LOCAL DIFFUSIVITIES

We assume that the distribution of the absolute displacements at short times has the exponential form

$$p(\mathbf{x}, t) = C(t) \exp(-a(t)|\mathbf{x}|),$$

with $a(t)$ defining the width of the distribution and $C(t)$ being the normalization constant. Requiring that

$$\int p(\mathbf{x}, t) d\mathbf{x} = 1$$

and that

$$\int p(\mathbf{x}, t) |\mathbf{x}|^2 d\mathbf{x} = 2dD_0t$$

in d dimensions, we obtain the explicit form of the displacements' PDFs

$$\begin{aligned} p(x, t) &= \frac{1}{2\sqrt{D_0t}} \exp\left(-\frac{x}{\sqrt{D_0t}}\right) & \text{in } d = 1 \\ p(\mathbf{x}, t) &= \frac{3}{4\pi D_0t} \exp\left(-\sqrt{\frac{3}{2}} \frac{x}{\sqrt{D_0t}}\right) & \text{in } d = 2 \\ p(\mathbf{x}, t) &= \frac{1}{\pi(2D_0t)^{3/2}} \exp\left(-\sqrt{2} \frac{x}{\sqrt{D_0t}}\right) & \text{in } d = 3 \end{aligned}$$

where $x = |\mathbf{x}|$.

The PDF of the particles' displacements at short times (i.e. in the superstatistical regime) is given by

$$p(\mathbf{x}, t) = \int_0^\infty \frac{1}{(4\pi dKt)^{d/2}} \exp\left(-\frac{r^2}{2dKt}\right) p_K(K) dK, \quad (12)$$

where K is what in the main text is called the "sampled diffusion coefficient". Passing to the Fourier transforms in the spacial coordinate and taking into account the central (rotational) symmetry of the PDF we get

$$\tilde{p}(\mathbf{k}, t) = \int_0^\infty \exp(-Ktk^2) p_K(K) dK,$$

and therefore see that $\tilde{p}(\mathbf{k}, t)$ is the Laplace transform of $p_K(K)$ taken at the value of the Laplace variable $s = tk^2$, and that $p(K)$ therefore follows as the corresponding inverse Laplace transform. The values of $\tilde{p}(\mathbf{k}, t)$ are

$$\tilde{p}(\mathbf{k}, t) = \begin{cases} \frac{1}{1 + D_0tk^2} & \text{in } d = 1 \\ \frac{1}{(1 + \frac{2}{3}D_0tk^2)^{3/2}} & \text{in } d = 2 \\ \frac{1}{(1 + \frac{1}{2}D_0tk^2)^2} & \text{in } d = 3 \end{cases}$$

and therefore $p(K)$ are the Γ -distributions

$$p(K) = \begin{cases} \frac{1}{D_0} \exp\left(-\frac{K}{D_0}\right) & \text{in } d = 1 \\ \frac{3^{3/2}}{\sqrt{2\pi}D_0} \sqrt{\frac{K}{D_0}} \exp\left(-\frac{3}{2} \frac{K}{D_0}\right) & \text{in } d = 2 \\ \frac{4}{D_0} \frac{K}{D_0} \exp\left(-2 \frac{K}{D_0}\right) & \text{in } d = 3, \end{cases} \quad (13)$$

i.e. possess the form

$$p(K) = \frac{\beta^\beta}{\Gamma(\beta)} \frac{1}{D_0} \left(\frac{K}{D_0}\right)^{\beta-1} \exp\left(-\beta \frac{K}{D_0}\right) \quad (14)$$

with the shape parameter $\beta = (d+1)/2$, with d being the dimension of space, and with the mean D_0 .

The first inverse moment of the distribution $\langle D^{-1} \rangle = D_0^{-1} \beta \Gamma(\beta-1) / \Gamma(\beta) = D_0^{-1} \beta / (\beta-1)$ diverges in $d = 1$ and is finite in higher dimensions:

$$\langle D^{-1} \rangle = \begin{cases} 3/D_0 & \text{in } d = 2 \\ 2/D_0 & \text{in } d = 3. \end{cases}$$

At short times we have essentially superstatistics: the particles move in different areas with different local diffusion coefficients $D(\mathbf{x})$. Since the patches do not have to be sampled homogeneously the distribution of sampled diffusion coefficients K might differ from such of D .

In equilibrated cases the area around \mathbf{x} is sampled with probability proportional to the local equilibrium concentration $n(\mathbf{x})$ of particles therein. In the case when

equilibrium distribution of particles over the system is homogeneous ($n(\mathbf{x}) = \text{const}$), i.e. under the Hänggi-Klimontovich interpretation, $p_D(D)$ and $p_K(K)$ coincide as well. The situation in other equilibrated cases is different, as discussed in the main text.

Since the equilibrium density in these cases is proportional to $D^{\alpha-1}(\mathbf{x})$, the normalization implies that

$$\nu(\mathbf{x}) = \frac{D^{\alpha-1}(\mathbf{x})}{\langle D^{\alpha-1}(\mathbf{x}) \rangle}. \quad (15)$$

In the case of homogeneous sampling the distribution of the local diffusion coefficients is given by $p_K(K)$, Eq.(13), which coincides with $p_D(D)$ as discussed before, from which the normalization constant $\tilde{N} = \langle D^{\alpha-1}(\mathbf{x}) \rangle^{-1}$ follows readily:

$$\tilde{N} = \frac{\beta^{\alpha-1} \Gamma(\beta)}{\Gamma(\beta + \alpha - 1)} D_0^{1-\alpha}.$$

The distribution of $\kappa = D^\alpha / \langle D^{\alpha-1} \rangle$ follows from $p_D(D)$ by the variable transformation.

In the equilibrated case the normalization constant in Eq.(15) cannot be given immediately, since the distribution of D is not yet known. However, since the dependence of ν on D is deterministic, we can write $\nu(\mathbf{x}) = N D^{\alpha-1}(\mathbf{x})$ and substitute this in Eq.(5) of the main text to get

$$\begin{aligned} p_D(D) &= N^{-1} D^{1-\alpha} p(D) \\ &= N^{-1} \frac{\beta^\beta}{\Gamma(\beta)} \frac{1}{D_0} \left(\frac{1}{D_0} \right)^{\beta-1} D^{\beta-\alpha} \exp\left(-\beta \frac{D}{D_0}\right), \end{aligned} \quad (16)$$

and require the normalization of the l.h.s. From this we get

$$N = \frac{\beta^{\alpha-1} \Gamma(\beta - \alpha + 1)}{\Gamma(\beta)} D_0^{1-\alpha}. \quad (17)$$

On the r.h.s. of Eq.(16) we recognize an “embryonic” Γ -distribution with the shape parameter $\beta' = \beta - \alpha + 1$ (as it is seen from the corresponding power of D in the pre-exponential), and with a mean D'_0 different from D_0 . This is given by $D'_0 / (\beta - \alpha + 1) = D_0 / \beta$ necessary to get the argument of the exponential function to be $-\beta' D / D'_0$, and is equal to

$$D'_0 = \frac{\beta - \alpha + 1}{\beta} D_0.$$

The corresponding parameters β' and D'_0 are then denoted by β and \bar{D} in Eq.(6) of the main text and in Eq.(18) below.

Thus, the PDFs of the local diffusion coefficients all cases are given by the Gamma distributions

$$p(D) = \frac{\beta^\beta}{\Gamma(\beta)} \frac{1}{\bar{D}} \left(\frac{D}{\bar{D}} \right)^{\beta-1} \exp\left(-\beta \frac{D}{\bar{D}}\right) \quad (18)$$

(as it follows from Eq.(14) for homogeneous sampling case and from Eq.(16) for the equilibrated case). In the HK case and in the Ito case for homogeneous sampling the parameters are $\beta = (d+1)/2$ and $\bar{D} = D_0$; in the equilibrated Ito case they are $\beta = \frac{d+1}{2} + 1 = (d+3)/2$ and $\bar{D} = \frac{\beta+1}{\beta} D_0 = \frac{d+3}{d+1} D_0$.

The cumulative distribution functions corresponding to PDFs Eq.(18) are

$$F_\beta(D) = \int_0^D p(D') dD' = \frac{1}{\Gamma(\beta)} \gamma\left(\beta, \beta \frac{D}{\bar{D}}\right) \quad (19)$$

with $\gamma(\alpha, x)$ being the lower incomplete Γ -function. This form will be used for generating diffusivity landscapes in simulations, as discussed in the next Section.

SIMULATIONS OF THE PDF AND MSD IN THE PURE DIFFUSION CASES

We start from a discretized model and consider the situation described by the master equation

$$\frac{d}{dt} p_i = \sum_j (w_{ij} p_j - w_{ji} p_i).$$

The corresponding equations can be considered as discretization of the corresponding Fokker-Planck equations, or follow as Master equations for the random walk schemes converging to the Langevin equation for corresponding interpretation of stochastic integrals. The transition rates will follow the distribution similar to the distribution of local diffusivities $p_D(D)$ given by Eq.(18); the local diffusivity for the rates which vary slowly in space will be $D = 2dw$.

For the HK case the rates $w_{ij} = w_{i \leftarrow j}$ satisfy the condition of the detailed balance, i.e., in the absence of the external force $w_{ij} = w_{ji}$ as discussed in Ref. [23] of the main text. The rates follow from the PDF $p(w)$ derived from such of D .

To simulate the Ito situations, we assume that the transition probabilities from each site to all its neighbors are the same, and it is the inverse waiting time which has the corresponding distribution. The transition rate from the site i to any of its neighboring sites j is $w_{ij} = w_i$ and this w_i is distributed according to the corresponding $p(w)$ (note that the rates are now defined not on the bonds, but for the sites of the lattice) [23]. The transitions now are asymmetric: $w_{ij} \neq w_{ji}$, which makes a difference. Then, for the case of homogeneous sampling, we repeat the same calculations we did for the symmetric bond disorder (HK case).

The master equation is solved numerically by forward Euler integration scheme to get $p_i(t)$ for each site i characterized by coordinates (k, l) and the numerically exact MSD $R^2(t)$ for the initial condition concentrated at the

origin is obtained as a function of time for each given realization of the random diffusivity landscape. In 2d the system is of the size $(2L+1) \times (2L+1)$ (i.e. one has $-L \leq k, l \leq L$). The MSD for a particle starting at the origin ($k = l = 0$) is then $R^2(t) = \sum_{k,l=-L}^L (k^2 + l^2) p_{(k,l)}(t)$. These exact MSDs are then averaged over different realizations of w_{ij} (typically 1500 realizations). In 3d the procedure is similar. In the equilibrated Ito case the corresponding probabilities and MSDs are weighted with the inverse transition rate from the origin w_0^{-1} , which is proportional to the equilibrium concentration.

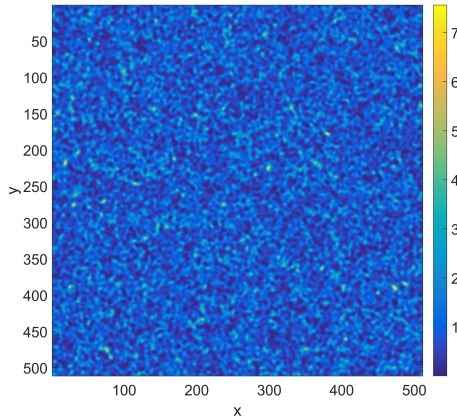


FIG. 4. A single realization of a landscape of diffusion coefficients with $\lambda = 10$ lattice units obtained by the method outlined.

The correlated random variables $w(\mathbf{x})$ can be easily obtained by a probability transformation.

Let us call $F_\beta^{-1}(x)$ the function inverse to $F_\beta(D)$, as given by Eq.(19). Then the probability transformation

$$w(z) = F_\beta^{-1} \left[\frac{1}{2} \operatorname{erfc} \left(\frac{z}{\sqrt{2}} \right) \right]$$

transforms the Gaussian variable z with zero mean and unit variance into a Γ -distributed w with necessary properties. The corresponding function $F_\beta(x)$ can be easily inverted (there exists a standard MATHLAB implementation for this inverse), and therefore the corresponding fields can be easily simulated for any given two-point correlation function. In our simulations we use independent Gaussian variables for the uncorrelated case, or a correlated Gaussian landscape with Gaussian correlation function $\langle z_i z_j \rangle = \exp(-r_{ij}^2 / 2\lambda^2)$ with r_{ij} being the distance between the sites i and j and λ being the correlation length, which is easily obtained by filtering of the initial array of independent Gaussian variables. The corresponding example of the diffusivity landscape is shown in Fig. 4.

The results of the corresponding simulations for the diffusivity $D(t) = \frac{d}{dt} \langle R^2(t) \rangle$ and for the PDF of the particles' positions are shown in Figs. 5 and 6.

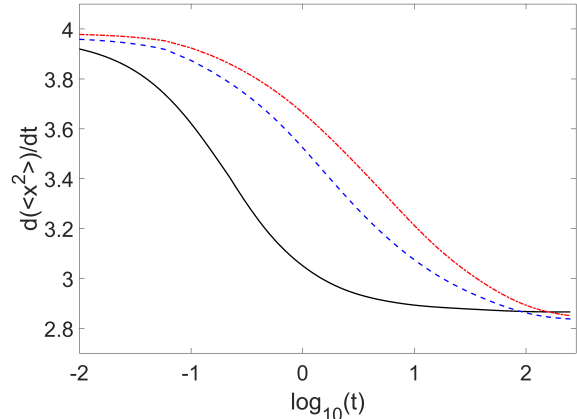


FIG. 5. Time dependent diffusion coefficients as obtained by numerical differentiation of MSD for diffusivity landscapes with different correlation lengths in $d = 2$ for an uncorrelated transition rates (solid black curve), and for diffusivity landscapes with correlation length $\lambda = 5$ (dashed blue line) and $\lambda = 10$ (red dashed-dotted line). The deviation of the curves in the limit of short times gives impression about the typical statistical error of simulation. The parameters of simulations imply $D_0 = \bar{D} = 4$. The simulation results reproduce the ones of EMA within a statistical accuracy (i.e. within a few percent). Thus the terminal diffusion coefficient for the uncorrelated case is $D^* = 2.87$ vs. EMA prediction of 2.88. As we see, the diffusion coefficient in this case is not constant over the time.

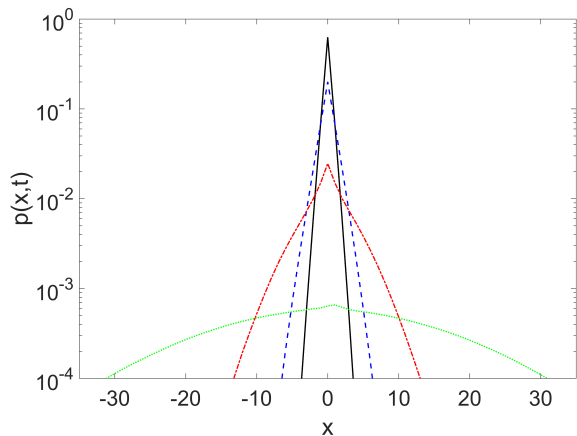


FIG. 6. The probability density functions of the displacements in projection on x axis for $\lambda = 10$ at different times: at a short time, in the transition regime and a very long times. The times are (from top to bottom) $t = 0.1, 1, 10$ and 200 . Note the logarithmic scale. The figure clearly demonstrates the transition between the double-sided exponential and the Gaussian form.

All figures presented in the main text and above are the ones for two-dimensional systems. The reason is that in 3d the systems are inevitably smaller, and achieving long times without running into finite size effects (espe-

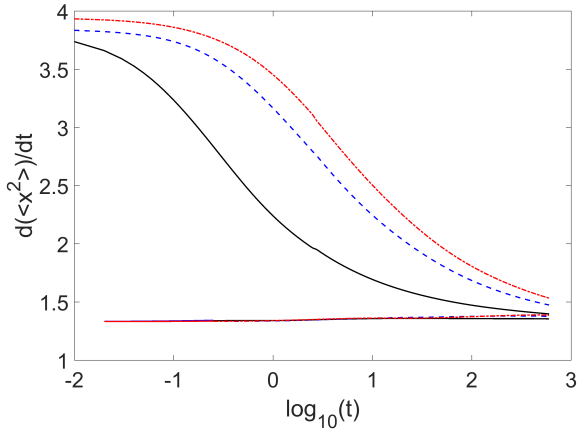


FIG. 7. Time dependent diffusion coefficients as obtained by numerical differentiation of MSD for diffusivity landscapes with different correlation lengths in $d = 2$ for the Ito case. The bunch of the curves starting at $D_0 = \bar{D} \approx 4$ corresponds to an ordinary situation and again shows the considerable decay of the diffusion coefficient with time. The theoretical estimate for the terminal diffusion coefficient is $D^* = D_0 \approx 1.33$, and approaching this value by the simulation results is evident. The lower bundle of curves corresponds to the equilibrated situation where theoretically $D_0 = D^* = \bar{D}/3$. The deviations from the constant diffusivity stay within the statistical error, which in the present case is larger than for the case of homogeneous equilibrium. The coding of the curves is the same as in Fig. 5.

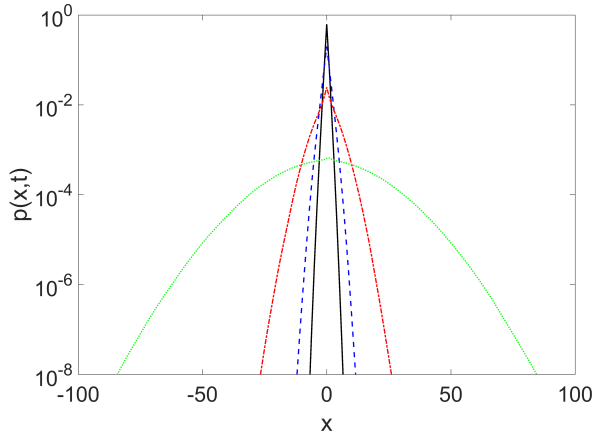


FIG. 8. The probability density functions of the displacements in projection on x axis for $\lambda = 10$ at different times for the ordinary Ito case. The times are (from top to bottom) $t = 1, 10, 100$ and 250 . Note the logarithmic scale. The transition between the double-sided exponential and the Gaussian form is demonstrated clearly.

cially for large values of λ) is problematic. To show that the behavior in $d = 3$ is similar we show, in the Figure 6 below, the results for the time dependent diffusion coefficient in $d = 3$ for $\lambda = 3$. The EMA prediction for the HK case corresponds to $D^*/D_0 \approx 0.852$ (as stated in the main text), and for the Ito case under homogeneous sampling the analytical prediction is $D^*/D_0 = 0.5$.

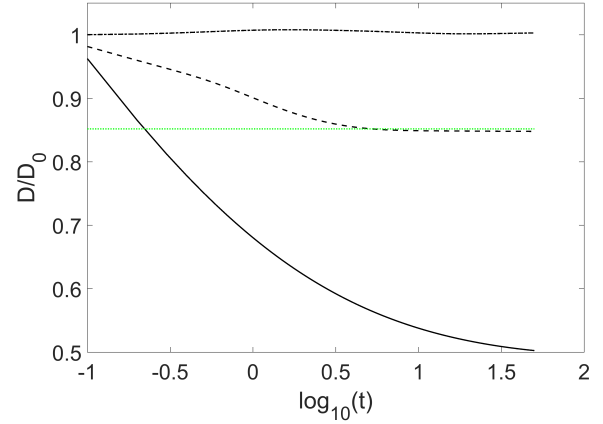


FIG. 9. The behavior of $D(t)/D_0$ for the HK case and the two Ito cases for the same value of $\lambda = 3$ in $d = 3$. The upper dashed-dotted line corresponds to the equilibrated Ito case and stays horizontal within the statistical error. The lower dashed line gives the time-dependent diffusion coefficient in the HK case. The lowest full line corresponds to the Ito situation under homogeneous sampling.